

Integrated Interpretation of 2D IP-Resistivity Data for Sulfide Mineral Exploration in Ameka, Lower Benue Trough, Southeastern Nigeria

L.O. Nwakpa, C. N. Okereke and F. B. Akiang

Department of Geology, Federal University of Technology Owerri, Nigeria

*Corresponding author: Luke Onyebuchi Nwakpa, Department of Geology, Federal University of Technology Owerri, Nigeria.

Citation: L. O. Nwakpa, C. N. Okereke, F. B. Akiang (2026) Integrated Interpretation of 2D IP-Resistivity Data for Sulfide Mineral Exploration in Ameka, Lower Benue Trough, Southeastern Nigeria. *J. Ear Sci Bio Int* 2(1): 1-10.

Received Date: May 03, 2026

Accepted Date: May 07, 2026

Published Date: May 12, 2026

Abstract

This study presents an integrated interpretation of 2D Electrical Resistivity Tomography (ERT) and Induced Polarization (IP) data for delineating Pb-Zn sulfide mineralization in Ameka, within the Lower Benue Trough, Southeastern Nigeria. Six dipole-dipole profiles, each 300 m long with 10 m electrode spacing, were acquired and inverted using RES2DINV to generate high-resolution resistivity and chargeability models. The results reveal distinct subsurface anomalies characterized by low resistivity (10–50 Ωm) and high chargeability (≥ 200 msec), indicative of disseminated sulfide mineralization. These anomalies are prominent in Profiles 1, 3, 4, and 6 at depths ranging from approximately 17 to 50 m, and are spatially associated with fractured and sheared zones within the Asu River Group. In contrast, Profiles 2 and 5 exhibit relatively high resistivity and low chargeability responses, suggesting compact, unfractured shale and absence of significant mineralization. The integration of resistivity and chargeability data demonstrates that mineralization is structurally controlled, occurring preferentially along fracture corridors and weak zones that act as conduits for hydrothermal fluid flow. The lateral continuity of conductive and highly chargeable zones, particularly between Profiles 4 and 6, indicates a persistent mineralized trend oriented approximately N–S to NW–SE. This study refines the subsurface model of Pb-Zn mineralization in the area and identifies high-priority targets for drilling and further exploration, highlighting the effectiveness of integrated ERT–IP techniques in mineral prospectivity mapping within sedimentary basins.

Keywords: Electrical Resistivity Tomography (ERT), Induced Polarization (IP), Pb-Zn mineralization, Chargeability; Resistivity, Lower Benue Trough, Asu River Group, Geophysical exploration, Structural control, Hydrothermal mineralization

Introduction

The Pb-Zn-barite mineralization of the Benue Trough spans the Lower, Middle, and Upper segments of the basin and constitutes one of the most significant metallogenic provinces in Nigeria. This mineralization belt extends from the Abakaliki-Ishiagu axis in the Lower Benue Trough, where it is hosted predominantly within Albian shale-limestone sequences, through the Arufu-Akwana-Azara district in the Middle Benue Trough characterized by Cenomanian limestone and marl, to the Zurak-Wase-Gwana areas of the Upper Benue Trough, where mineralization is associated with the Bima and Yolde Formations. These occurrences define three principal Pb-Zn mineralization districts within the trough.

Despite the economic importance of these mineral resources, exploration and exploitation activities within many parts of the basin remain largely underdeveloped and poorly constrained. In several localities, including the Ameka area of southeastern Nigeria, uncertainties persist regarding the depth, lateral continuity, and structural controls of sulfide mineralization. This lack of reliable subsurface information has contributed to inefficient exploration practices, informal mining activities, and suboptimal resource management. Consequently, there is a critical need for detailed and systematic subsurface investigations to improve target delineation and reduce exploration risk.

Geophysically, sulfide mineralization such as galena (PbS) and sphalerite (ZnS) is often associated with distinct electrical signatures, making integrated geophysical methods particularly effective for their detection. In particular, electrical resistivity and induced polarization (IP) techniques have proven useful in identifying disseminated sulfide zones due to their sensitivity to variations in subsurface conductivity and chargeability. The application of two-dimensional (2D) imaging further enhances the resolution of subsurface features, enabling improved delineation of mineralized zones and associated structural controls.

Lead (Pb) is a dense, soft, bluish-grey metal that primarily occurs in nature as galena (PbS), often in association with sphalerite (ZnS) and barite (BaSO₄). Galena may also contain trace amounts of silver, making it an important secondary source of this metal. Zinc (Zn), on the other hand, is typically mined as sphalerite, which may contain trace elements such as cadmium, gallium, germanium, and indium. Barite, a barium sulfate mineral, commonly occurs in hydrothermal vein systems and is frequently associated with Pb–Zn mineralization within carbonate host rocks [1].

Given the geological complexity and economic significance of Pb–Zn mineralization within the Benue Trough, this study applies 2D electrical resistivity and induced polarization imaging to investigate subsurface characteristics of the Ameka area. The aim is to delineate potential mineralized zones, estimate their depth of occurrence, and evaluate the structural framework controlling mineral deposition. The outcomes of this research are expected to contribute to more efficient exploration strategies and provide a geophysical basis for targeted mineral development in the region.

Location and Accessible, Physiography and Geology of the study area

Ameka area is located in at Ezza South local Government Area of Ebonyi State, the study area is bounded by Latitude 6°03'2"00"-N6°17'00"N of the Equator and Longitude 7°59' 00" E - 8° 13' 00"E of the Greenwich Meridian. The area is accessible through Express way, major roads, minor roads and footpaths. The access route include: Abakaliki Afikpo Expressway, Abakaliki-Ikwo road and Ikwo Ameka road. The area can also be accessed through Onueke-Ameka Road. Most of the sites visited for data acquisition were accessed by vehicle, motorcycle, and foot. The footpaths formed the major conduit to the virgin areas. While areas with ongoing mining activities were accessed with motorcycles and vehicles. Figure 1, shows the accessibility map of the study area.

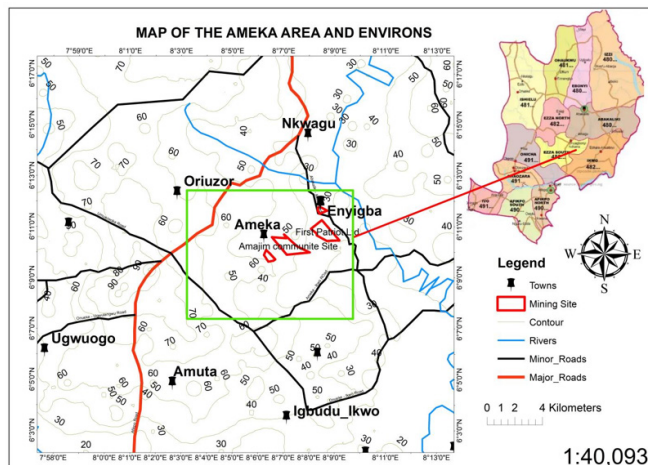


Figure 1: Accessibility Map of Ameka area and Environs

Ameka Southeastern Nigeria is underlain by the Lower Benue Trough, which lies within the Cross River plains and the Abakaliki anticlinorium, a physiographic zone dominated by undulating hills, low-lying plains, and structurally controlled ridges. Elevations generally range from 15 to 120m above sea level, with rugged terrain in the northeast near Enyigba Northeastern part and more gently sloping Oriuzor. The physiography is a direct reflection of the underlying geology, where resistant shale units form ridges, while softer siltstones and alluvial deposits occupy valleys towards the south and southeastern part, around Ikwo area (figure 2). The undulation has greatly increased in recent years. due to incessant mining activities around the area by artisans.

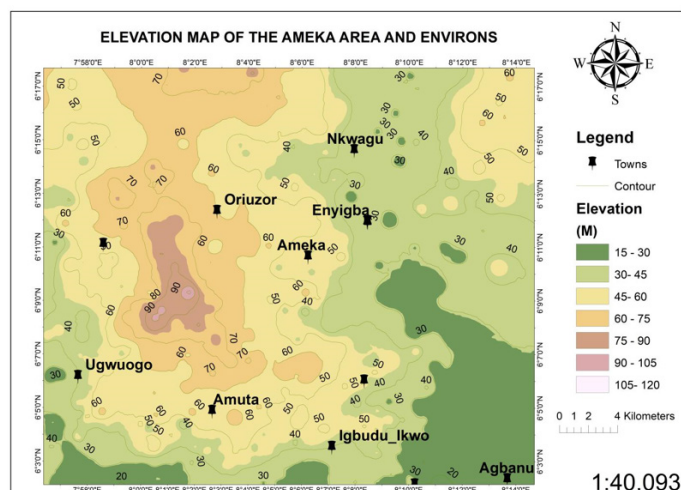


Figure 2: Elevation Map of the Study area

The Geology of the area, Ameka area lies within the Lower Benue Trough, a rift-related sedimentary basin that developed

during the opening of the South Atlantic in the Early Cretaceous. The stratigraphic succession in this region comprises Albian to Maastrichtian sediments, intruded locally by Santonian pyroclastics and mineralized veins. The lithostratigraphy of the area includes the Asu River Group, Eze-Aku Formation, Awgu Formation, and post-Santonian sediments [2-5].

The Asu River Group represents the oldest sedimentary unit in the study area, deposited during the Albian transgression. It consists predominantly of shales, siltstones, sandstones, and occasional limestone interbeds. The shales are dark grey to black, fissile, and pyritic, often associated with organic matter, making them potential hydrocarbon source rocks. These rocks are also the primary hosts of lead-zinc mineralization in the Lower Benue Trough, with sulfide veins emplaced along fractures and faults [2-3, 6].

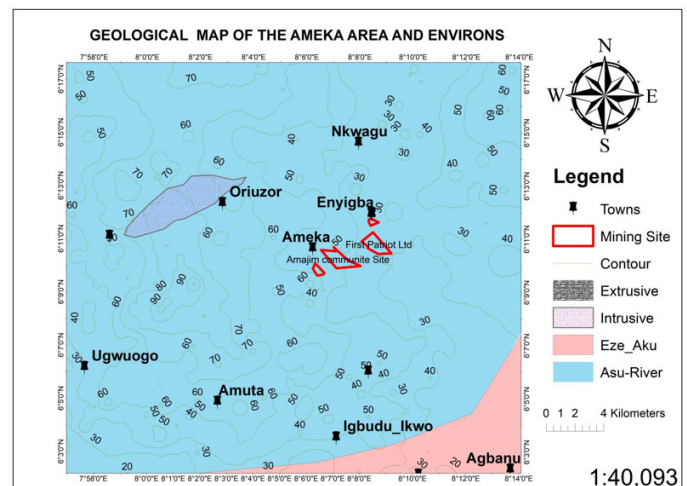


Figure 3: Geological Map of the study area

Materials and Methods

Data Acquisition

This study adopts a hybrid geophysical approach integrating Electrical Resistivity Tomography (ERT) and Induced Polarization (IP) methods within a Geographic Information System (GIS) framework. The integration of these methods enhances subsurface imaging resolution, reduces interpretational ambiguity, and improves delineation of Pb-Zn mineralization targets. Six (6) 2D ERT/IP profiles were acquired using a Geomatic GD-10. The system was configured with 30 electrodes at 10 m spacing, resulting in a profile length of 300 m per line. Data were collected using a dipole-dipole array configuration to optimize lateral resolution and depth of investigation. Profiles were oriented in the East-West (E-W) direction, perpendicular to regional NE-SW and NW-SE structural trends interpreted from existing geological and geophysical datasets.

Field Procedures

Data acquisition followed a systematic workflow to ensure consistency and data quality:

1. Site Selection and Preparation

Survey locations were selected based on accessibility, minimal surface disturbance, and suitability for linear profile deployment. Each traverse was cleared where necessary to ensure straight-line electrode layout in the E-W direction.

2. Electrode and Porous Pot Installation

Stainless steel electrodes (40 cm length) were installed at 10 m intervals. Porous pots filled with copper sulphate solution were inserted into the same electrode holes to enhance electrochemical stability and minimize polarization effects during IP measurements.

3. Cable Layout and System Setup

Multi-core 2D cables connected all electrodes to the Geomatic GD-10 system, enabling automated switching and synchronized acquisition of resistivity and induced polarization data.

4. GPS Survey and Georeferencing

Precise coordinates of all electrode positions were recorded using a handheld GPS unit. These coordinates were used for georeferencing, spatial referencing, and subsequent GIS integration of the inverted geophysical models.



Figure 4: Electrode and porous pot installation in progress. (a) shows the connection, while (b) shows already installed Electrode and porous pot connected to 2D cable.

The resistivity and induced polarization method involves the measurement of electrical impedance, with subsequent interpretation in terms of subsurface electrical properties and, in turn, subsurface geology. These methods utilize artificial means to introduce current into the ground and measure the resulting potential difference within the vicinity of current flow [9].

In a completely homogeneous ground, the resistivity measured would be the true resistivity and would remain constant for any current and electrode arrangement. However, the Earth's subsurface is inherently inhomogeneous; as a result, the measured resistivity varies with changes in electrode configuration and position, giving rise to what is termed apparent resistivity [7-8]. Knowledge of typical resistivity values for different subsurface materials, along with an understanding of the local geology, is essential for accurate data interpretation [10].

Induced polarization (IP) makes use of the capacitive properties of subsurface materials to temporarily store electrical charge. The primary advantage of this method is its ability to detect disseminated metallic minerals by exploiting two mechanisms of electrical current flow in the subsurface: electronic conduction and electrolytic conduction. Metallic sulphide minerals, in particular, facilitate electronic conduction [9, 7].

When a steady current is introduced into the ground through a pair of electrodes and subsequently switched off, the measured voltage does not immediately drop to zero but instead decays gradually over time. This observed voltage consists of the primary voltage due to the applied current and a secondary polarization voltage resulting from charge accumulation within the subsurface materials [9]. In the absence of polarizable materials, this decay voltage is negligible or zero. The integration of the decaying voltage over time defines the decay curve, and the parameter derived from this process is referred to as the apparent chargeability [10].

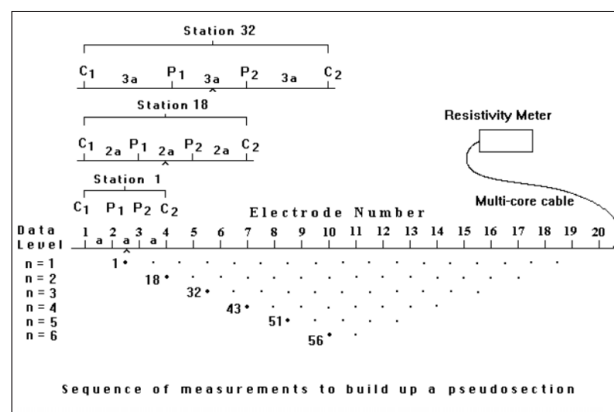


Figure 5: 2D layout with pseudo-section [10]

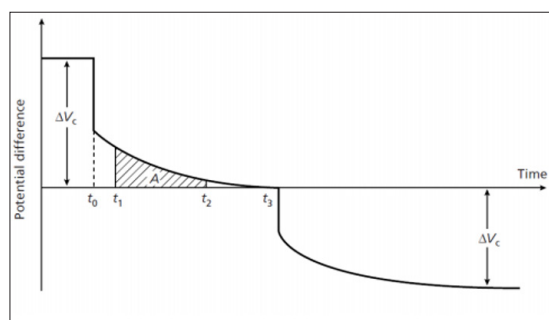


Figure 6: The phenomenon of induced polarization. At time t_0 , the current is switched off and the measured potential difference, after an initial large drop from the steady-state value ΔV_c , decays gradually to zero. A similar sequence occurs when the current is switched on at time t_3 . A represents the area under the decay curve for the time increment t_1-t_2 [10].



Figure 7: 2D IP/Resistivity Data Acquisition in Progress after equipment set up.

Software and Tools

RES2DINV (Geotomo) for inversion and section plotting. ArcMap 10.8 / ArcGIS Pro 3.0 for georeferencing, Maps digitization, and integrating resistivity sections into GIS. Microsoft Excel and Note Pad for Pre-processing of resistivity data. Microsoft Word for Technical reporting.

Data Processing

The data acquired from the profiles using the Dipole - Dipole array, were processed and inverted using RES2DINV, a widely used 2D resistivity/IP inversion software. Both resistivity and IP

measurements were recorded simultaneously, employing porous pot electrodes inserted into 6-inch-deep holes, ensuring consistent ground coupling. This process converts the raw voltage differences into quantitative subsurface resistivity and chargeability models, which are essential for delineating Pb-Zn sulfide mineralization zones.

Data Quality Check

Raw field data are first examined for errors such as spikes, negative apparent resistivity, and inconsistent measurements. Measurements with excessively high standard deviation or low signal-to-noise ratio are removed. Electrode contact resistances are reviewed to ensure proper coupling with the ground.

Geometric Factor Application

The apparent resistivity (ρa) is calculated from measured potential differences using the dipole–dipole geometric factor, K :

$$\rho a = K \cdot \frac{\Delta V}{I} \quad (1)$$

Where ΔV is the potential difference, I is the current, and K depends on electrode spacing and array configuration.

Correction of IP Data

IP data are corrected for electrode polarization and instrumental drift.

Chargeability (M) is computed as:

$$M = \frac{\sum \Delta V(t) \cdot \Delta t}{V_p \cdot \sum \Delta t} \quad (2)$$

Where $\Delta V(t)$ is the voltage decay over time and V_p is the primary voltage.

Stacking and Filtering

Multiple measurements at the same electrode configuration were stacked to reduce random noise. Low-pass or moving average filters were applied to smooth the data while preserving significant anomalies.

Generation of Pseudo-sections

Apparent resistivity and chargeability values were plotted against electrode positions to produce 2D pseudo-sections. Pseudo-sections provided a first-order visualization of lateral and vertical variations, helping to identify areas of high chargeability (potential sulfide zones) and high/low resistivity contrasts.

Inversion Using RES2DINV

The RES2DINV software uses a smoothness-constrained least-squares algorithm to convert apparent resistivity and chargeability pseudosections into 2D subsurface models. The inversion workflow included:

Model Initialization

The subsurface was discretized into rectangular blocks along the 2D profile. Initial resistivity and chargeability values were assigned based on the known geology of Oshiri and Ameka. The dipole–dipole array configuration was specified to match field acquisition.

Forward Modeling and Iteration

RES2DINV calculated the theoretical apparent resistivity for the initial model. Misfit between observed and calculated data was minimized iteratively using the software's inversion algorithm. Inversion iterations continued until convergence criteria were met, typically when the root mean square (RMS) is low.

Constraints and Parameter Settings

Smoothness constraints were applied laterally and vertically to avoid unrealistic resistivity variations. Depth-dependent weighting was included to compensate for reduced sensitivity at greater depths. IP inversion utilized a similar approach, producing 2D chargeability sections aligned with resistivity anomalies.

Generation of 2D Models and Pseudo-sections

The final 2D resistivity and chargeability models were visualized as color-coded pseudo-sections. Low resistivity combined with high chargeability was interpreted as potential Pb -Zn sulfide mineralization, whereas high resistivity zones corresponded to quartz veins or barren host rocks.

Constraints and Considerations

Smoothness constraints were applied to prevent unrealistic variations between adjacent blocks. Depth-dependent weighting was incorporated to account for reduced sensitivity of deeper measurements. The 2D inversion assumed lateral homogeneity perpendicular to the profile; complex 3D structures were interpreted cautiously.

Integration with GIS

Inverted models were exported to GIS for overlay with geological maps, structural features, and other geophysical datasets (figure 13). This integration aids in the delineation of target areas for detailed mineral exploration.

Results Presentation and Interpretation

The following section presents the interpretation of six (6) 2D Electrical Resistivity Tomography (ERT) and Induced Polarization (IP) profiles acquired across the study area. Each profile was analysed through integrated resistivity and chargeability inversion models generated using smoothness-constrained least-squares inversion to delineate subsurface electrical property distributions. Interpretation is based on the diagnostic relationship between resistivity and chargeability responses, where coincident low resistivity (typically $<50 \Omega\text{m}$) and elevated chargeability (≥ 200 msec) are indicative of disseminated sulphide mineralization, while high resistivity and low chargeability responses are associated with competent, unmineralized lithologies. The profiles are discussed individually to highlight lateral and vertical variations in subsurface electrical properties, with emphasis on identifying structurally controlled zones such as fractures and shear systems within the Asu River Group. These structures are evaluated as potential conduits for hydrothermal fluid flow and sulphide emplacement within the study area.

Profile 1

Profile 1 was acquired in an East-West (E-W) direction using 30 electrodes at 10 m spacing, giving a total profile length of 300 m and a maximum investigation depth of approximately 75 m. The resistivity section reveals a low-resistivity zone ($<30\text{-}50 \Omega\text{m}$) occurring between approximately 9 and 36 m depth, and laterally between 100 and 140 m along the profile. This conductive zone is spatially associated with high chargeability values, indicating the presence of disseminated sulphide mineralization (Figure 8). The coincident low resistivity and high chargeability response suggests that the anomaly is not clay-controlled but rather associated with a mineralized vein system hosted within fractured shale of the Asu River Group. The principal mineralized interval is interpreted between 17 and 36 m depth.

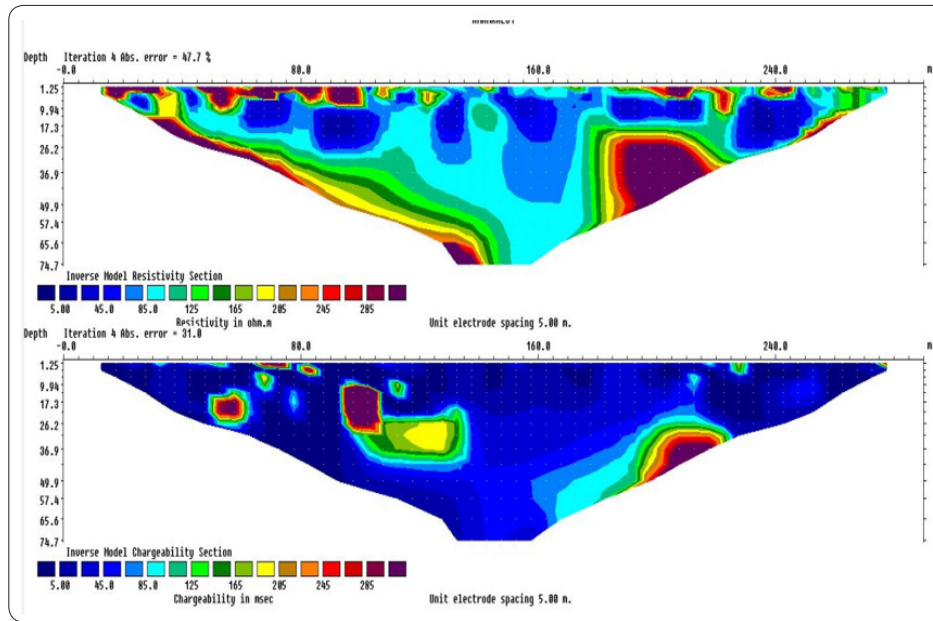


Figure 8: 2-D IP/Resistivity Profile map from location one

Profile 2

Profile 2 was also acquired along an E–W line with similar acquisition parameters (30 electrodes, 10 m spacing, 300 m length, and ~75 m depth of investigation).

The resistivity model is characterized by dominantly high values ($>250 \Omega\text{m}$) across approximately 90% of the profile length, indicating a relatively compact and unfractured shale sequence. Chargeability values remain low throughout the profile, suggesting the absence of significant disseminated sulphide mineralization.

This profile is therefore interpreted as a barren or weakly mineralized zone with minimal structural disruption.

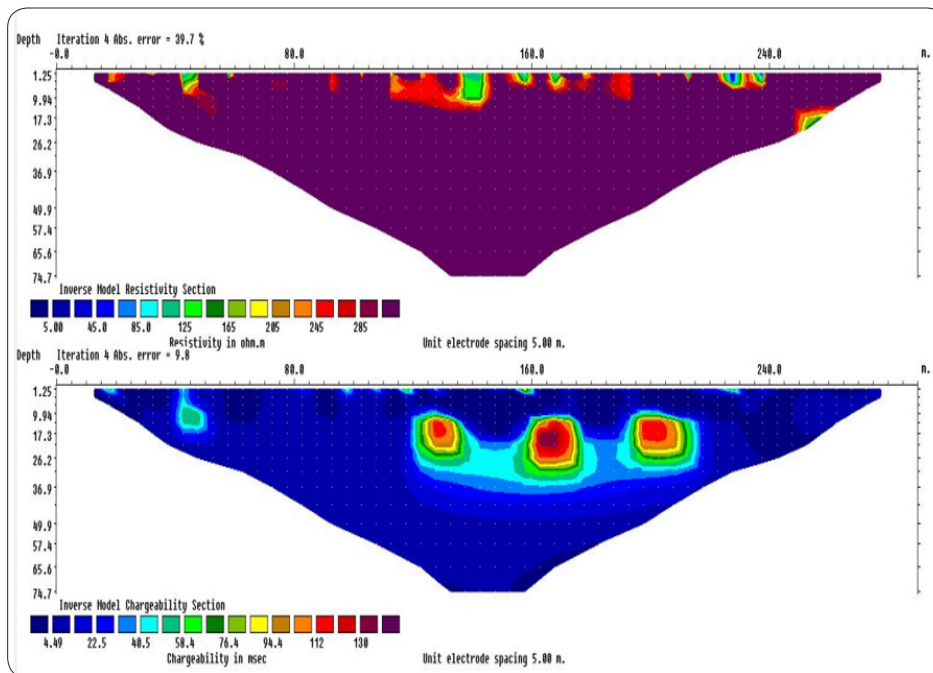


Figure 9: 2-D IP/Resistivity Profile map from location two

Profile 3

Profile 3, with a maximum depth of approximately 65 m, shows a progressive increase in resistivity from west to east, reflecting a transition from fractured to more competent shale units.

A distinct high chargeability anomaly ($>200 \text{ msec}$) occurs at depths between 26 and 50 m, particularly between 80 and 100 m along the profile. This anomaly coincides with a structurally disturbed zone, suggesting that mineralization is controlled by fractures and shear zones.

The spatial association of high chargeability and moderate-to-low resistivity supports the interpretation of disseminated sulphide mineralization within fractured shale horizons.

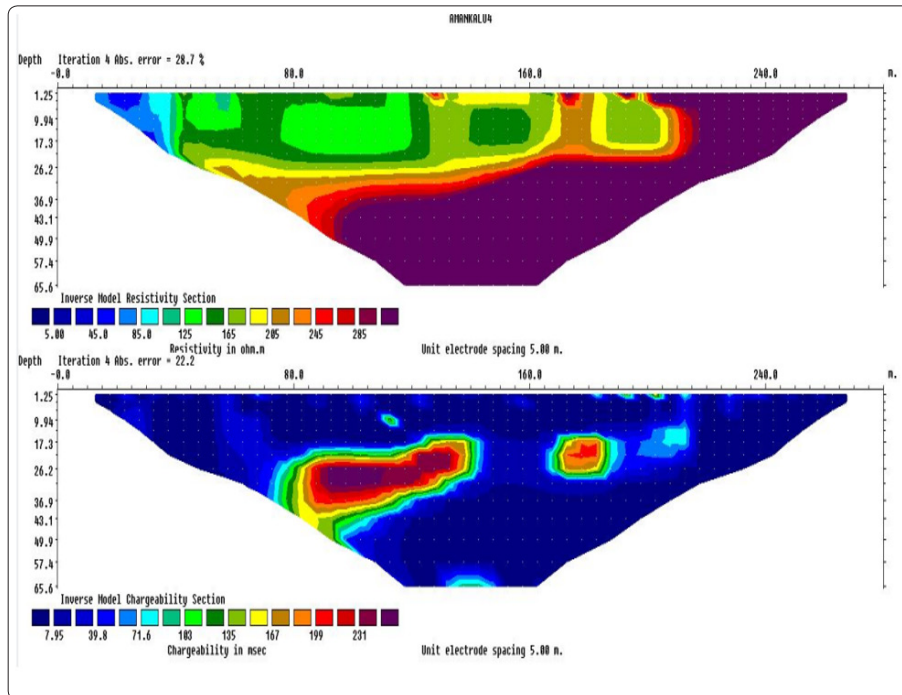


Figure 10: 2-D IP/Resistivity Profile map from location three

Profile 4

Profile 4 exhibits a heterogeneous resistivity structure characterized by a thin lateritic overburden (>200 Ωm) overlying a thick conductive zone (<30 Ωm) extending between 9 and 26 m depth.

This conductive unit is associated with consistently high chargeability values between 10 and 30 m depth, indicating the presence of sulphide mineralization rather than clay-rich materials.

The coincidence of low resistivity and high chargeability suggests that this zone represents a structurally controlled mineralized vein system within fractured shale, making it one of the most prospective zones in the study area.

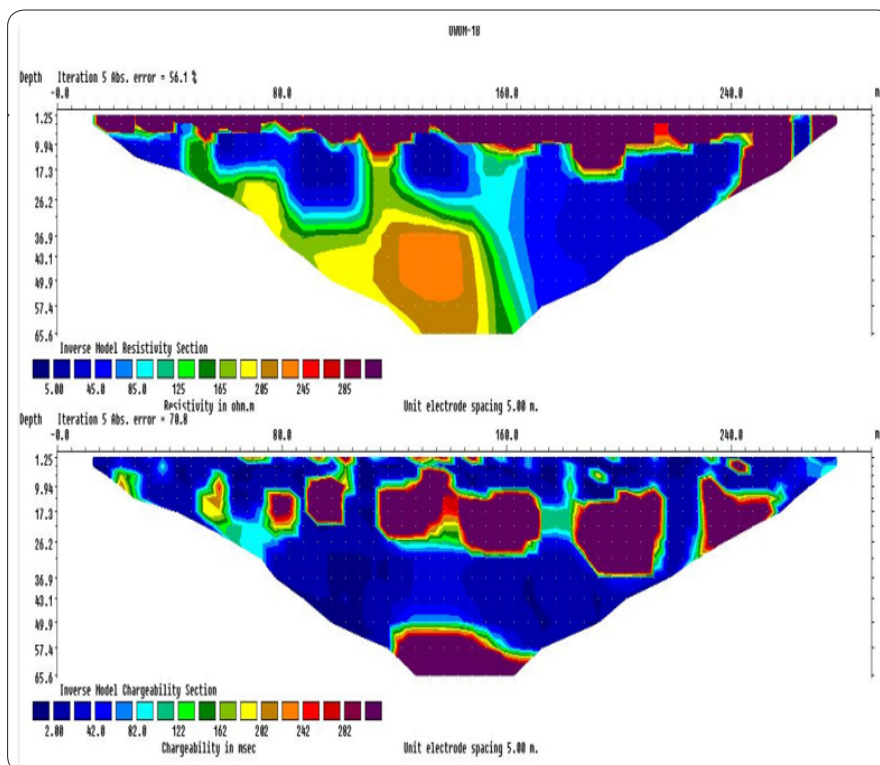


Figure 11: 2-D IP/Resistivity Profile map from location four

Profile 5

Profile 5 shows relatively high resistivity values (>425 Ωm) at deeper levels, indicating compact and competent shale. Shallow sections exhibit lower resistivity associated with the weathered overburden (figure 12). Chargeability values remain very low across the profile, indicating an absence of significant sulphide mineralization. This suggests that although the area may be structurally competent, it is not mineralized and likely represents barren shale within the Asu River Group sequence.

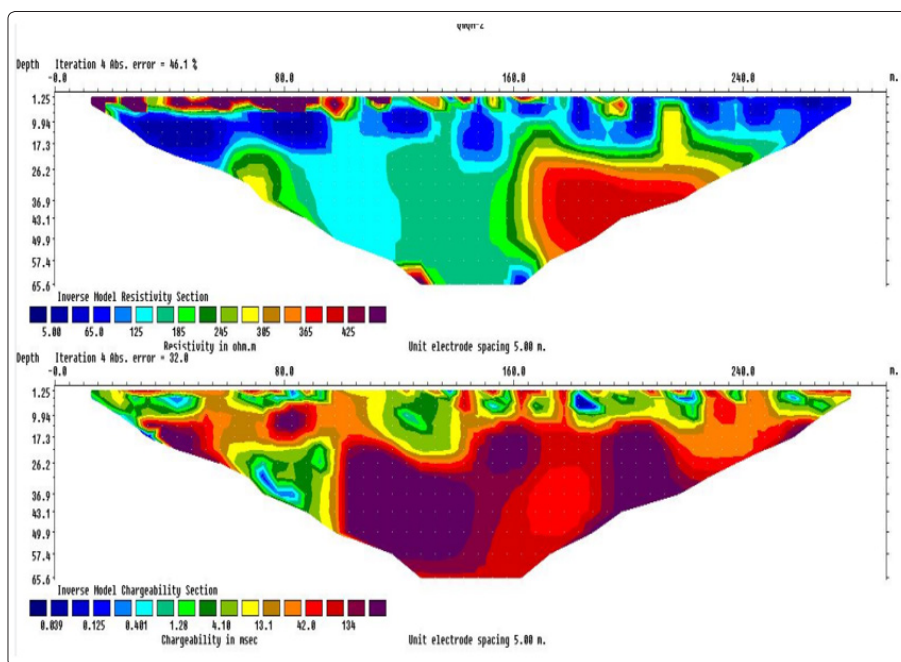


Figure 12: 2-D IP/Resistivity Profile map from location Five

Profile 6

Profile 6 was acquired under similar acquisition parameters and reveals a thick low-resistivity zone (<30 Ωm) extending from approximately 9 m to beyond 60 m depth (Figure 13). This conductive zone coincides with high chargeability values (>200 msec) between 26 and 50 m depth, indicating the presence of disseminated sulphide mineralization. The continuity of this anomaly suggests a structurally controlled mineralized corridor within fractured shale, consistent with a fracture system that facilitates hydrothermal fluid flow.

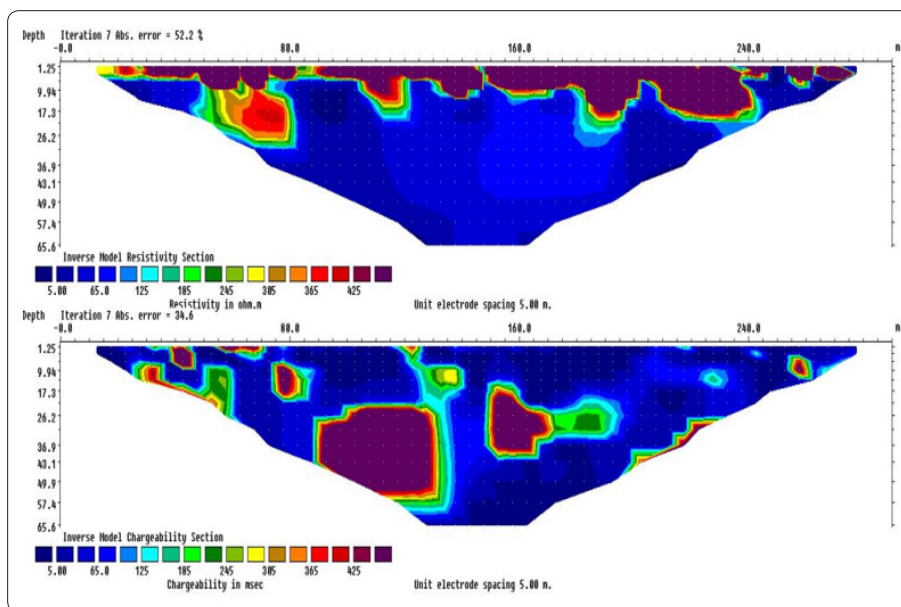


Figure 13: 2-D IP/Resistivity Profile map from location Six

IP/Resistivity Integration in GIS Environment

The six (6) 2D IP/Resistivity profiles obtained from the study area were integrated within a Geographic Information System (GIS) environment (Figure 14) using georeferenced coordinates acquired during field data collection. This integration enables accurate spatial representation and improved visualization of subsurface geophysical variations across the study area.

The combined interpretation of the resistivity and chargeability models reveals that the northeastern to southeastern and southern parts of the study area exhibit higher prospectivity for Pb–Zn mineralization. These zones correspond to Amajim (Ezza South), Ohankwu (Ikwo), Enyigba (Izzi), and Ameri (Ikwo), which are characterized by significant mining activities and known mineral occurrences.

Notably, these areas host several active mining operations, including First Patriot Nigeria Limited, one of the major mining companies operating in southeastern Nigeria. The spatial clustering of geophysical anomalies within these zones suggests strong structural control on mineralization and confirms the effectiveness of integrated ERT–IP and GIS-based approaches for mineral prospectivity mapping.

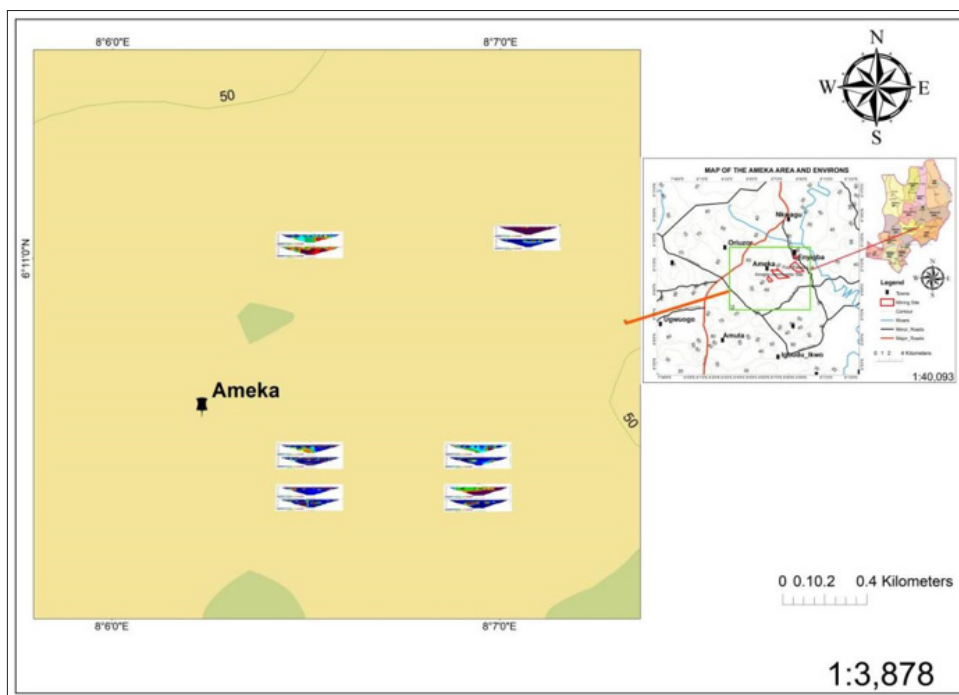


Figure 13: Integration of 2D IP/Resistivity profile in GIS Environment

Results Discussion

Array and Model Discretization

The Six profiles obtained in the study area were all processed and inverted in RES2DINV environment. Although the field data were acquired using a dipole-dipole array with an electrode spacing of 10m, the inversion carried out in RES2DINV employed an automatically refined model discretization. The software subdivides the electrode spacing into smaller computational cells (in this case ~5m, figure 8 to 13) to enhance inversion stability and improve subsurface resolution. This does not imply a change in acquisition geometry but reflects the numerical modelling approach used during inversion. The RES2DINV program uses a more sophisticated algorithm to subdivide the subsurface where the distribution of the model blocks is loosely tied to the data points in the pseudosection [10].

Subsurface Resistivity Distribution of the Study Area

The inversion results (Figures 8 -13) reveal variations in subsurface resistivity across the six profiles, reflecting lithological heterogeneity and structural complexity within the study area.

Profile One

Profile One, located in the northern part of Enyigba Izzi (Figure 8), reveals three major geoelectric layers. The near-surface layer exhibits resistivity values ranging from approximately 285 to 300 Ωm , interpreted as lateritic to moderately weathered materials. This layer is underlain by a conductive zone with resistivity values below 50 Ωm , which is interpreted as fractured, sheared, or clay-rich shale of the Asu River Group. A deeper resistive unit (>100 Ωm) is observed beneath this conductive zone and is interpreted as relatively competent or thermally altered (“baked”) shale. Low resistivity zones are commonly associated with clay content, fluid saturation, or structural deformation such as fracturing [8].

Profile Two

Profile Two (Figure 9), located in the northeastern part of the study area, exhibits a relatively uniform resistivity distribution, suggesting a more homogeneous subsurface. Two primary layers are identified: a thin overburden (approximately 2 m thick) and an underlying shale unit. Resistivity values range between 100 and 285 Ωm , indicating moderately consolidated shale with minimal structural disturbance. The absence of pronounced conductive anomalies suggests limited fracturing or fluid saturation along this profile [7].

Profile Three

Profile Three, located in Amogwee area (Figure 10), reveals three distinct geoelectric units. A thin surface layer (>200 Ωm) overlies a conductive zone (<50 Ωm) at the beginning of the profile, interpreted as a localized shear or fracture zone within the shale sequence. Toward the end of the profile, resistivity increases (160-300 Ωm), suggesting more competent and less fractured shale. Such lateral resistivity variation indicates structural heterogeneity, which may control fluid migration pathways within the formation [9].

Profile Four

Profile Four, located near Amajim community close to an active mining site, reveals three major layers. The upper layer (>200 Ωm) varies in thickness from approximately 7 m to over 10 m, indicating an undulating lateritic overburden. This is underlain by a thick conductive layer (<40 Ωm) with an approximate thickness of 20 m, interpreted as highly fractured or clay-rich shale. The deeper layer exhibits variable resistivity, ranging from about 200 Ωm to below 50 Ωm toward the end of the profile, suggesting

increasing fracturing or fluid saturation with depth. The presence of thick conductive zones near known mining activity may indicate structurally controlled zones that could serve as pathways for mineralizing fluids [9]

Profile Five

Profile Five exhibits a highly heterogeneous resistivity structure, indicative of a multi-fractured subsurface environment. The near-surface layer (approximately 5 m thick) shows resistivity variations from $>400 \Omega\text{m}$ to about $60 \Omega\text{m}$, suggesting lateral variability in weathering and fracturing intensity. The second layer ($<30 \Omega\text{m}$) is interpreted as a conductive zone associated with clay-rich or fluid-saturated fractured shale. The deeper unit ($125\text{--}300 \Omega\text{m}$) represents relatively competent shale. Such heterogeneity is characteristic of structurally complex zones, where multiple fractures enhance permeability and may facilitate the migration of mineralizing fluids [7].

Profile Six

Profile Six, located approximately 500 m from Profile Five, confirms the structural trend observed in the area. The near-surface layer exhibits high resistivity ($\sim 480 \Omega\text{m}$) with thickness ranging from 7 to 10 m, interpreted as lateritic overburden. This is underlain by a thick conductive zone ($<50 \Omega\text{m}$) extending to depths exceeding 70 m. This layer is interpreted as extensively fractured shale within the Asu River Group. The lateral continuity of this conductive zone between Profiles Five and Six suggests a persistent structural feature, possibly a fracture corridor or shear zone, which may act as a conduit for hydrothermal fluid flow.

Preliminary Interpretation from Resistivity

The resistivity models delineate lithological variations and structurally weak zones such as fractures and shear zones within the study area. These features are particularly evident in Profiles 4, 5, and 6, where laterally continuous conductive zones suggest structurally controlled pathways.

However, resistivity alone is not sufficient to uniquely identify sulphide mineralization, as low resistivity values may also result from clay-rich zones or fluid saturation. Therefore, while these conductive zones represent potential targets, confirmation requires integration with induced polarization (chargeability) data [10, 7]. The identified conductive zones, particularly those with structural continuity, are interpreted as favourable zones for mineralization and will be further evaluated using chargeability data.

Subsurface Chargeability Distribution of the Study Area

The inversion results (Figures 8-13) reveal significant variations in subsurface chargeability across the six profiles, reflecting the distribution of polarizable materials within the study area. Chargeability is particularly sensitive to disseminated metallic sulphides due to their ability to store electrical charge through electronic conduction mechanisms [9, 7]. The integration of chargeability with resistivity data enables discrimination between conductive clay-rich zones and zones of sulphide mineralization.

Profile One

Profile One, located in the northern part of Enyigba Izzi (Figure 8), exhibits a clear relationship between resistivity and chargeability distribution. The near-surface layer shows low chargeability values ($<50 \text{ msec}$), corresponding to high resistivity ($285\text{--}300 \Omega\text{m}$), and is interpreted as lateritic overburden. At depths between approximately 12 and 36 m, a pronounced high chargeability zone (216 to $>300 \text{ msec}$) is observed. This zone coincides with a low resistivity layer ($<50 \Omega\text{m}$), previously interpreted as fractured or clay-rich shale of the Asu River Group. The coexistence of low

resistivity and high chargeability strongly suggests the presence of disseminated sulphide mineralization rather than clay alone. This is because clay-rich materials typically exhibit low chargeability, whereas sulphide minerals produce significant polarization effects [9]. This zone is therefore interpreted as a potential mineralized target, warranting further investigation through drilling or trenching.

Profile Two

Profile Two (Figure 9), located in the northeastern part of the study area, shows a mixed chargeability response characterized by localized (high) values ($>250 \text{ msec}$) surrounded by low background values ($<30 \text{ msec}$). The high chargeability zones occur at depths between approximately 9 and 30 m and show similarities to the anomaly observed in Profile One. However, unlike Profile One, these anomalies are not strongly associated with low resistivity zones, as resistivity values range between 100 and $285 \Omega\text{m}$. This suggests that while polarizable materials may be present, the structural control (e.g., fracturing) appears less pronounced. Since resistivity does not indicate a well-developed conductive pathway, the mineralization potential in this profile remains uncertain and requires confirmation through ground truthing such as core drilling [7].

Profile Three

Profile Three (Figure 10), located in Amogwee, exhibits a distinct chargeability anomaly concentrated in the (central) part of the profile. Chargeability values range from approximately 125 to 250 msec at depths between 17 and 40 m. This anomaly spatially correlates with a conductive zone ($<50 \Omega\text{m}$) identified in the resistivity model, interpreted as a fracture or shear zone within the shale sequence. Toward the end of the profile, resistivity increases ($160\text{--}300 \Omega\text{m}$), while chargeability decreases significantly ($20\text{--}50 \text{ msec}$), indicating competent, unfractured, and non-mineralized shale. The spatial coincidence of high chargeability and low resistivity within a structurally weak zone suggests that mineralization is controlled by fractures and shear zones. This interpretation is consistent with field observations, including the presence of an active mining pit approximately 500 m from the profile, and supports the structurally controlled nature of Pb-Zn mineralization in the area.

Profile Four

Profile Four, located near Amajim community close to an active mining site, exhibits the most significant chargeability response in the study area. High chargeability values occur from shallow depths ($\sim 5 \text{ m}$) and extend downward through the conductive zone identified in the resistivity model. This zone corresponds to a thick conductive layer ($<40 \Omega\text{m}$) with an approximate thickness of 20 m, previously interpreted as fractured shale. However, the presence of consistently high chargeability within this conductive zone indicates that it is more likely associated with sulphide mineralization rather than clay-rich material. The coincidence of high chargeability and structural weakness suggests that this zone acts as a mineralization conduit, facilitating the movement and deposition of hydrothermal fluids. This interpretation aligns with established models where sulphide mineralization is structurally controlled within sedimentary basins [9]. This profile represents a high-priority exploration target.

Profile Five

Profile Five exhibits a highly heterogeneous resistivity structure indicative of a multi-fractured environment. However, the chargeability response is relatively low ($<200 \text{ msec}$), despite the presence of conductive zones ($<30 \Omega\text{m}$). This indicates that the conductive zones are more likely associated with clay-rich

or fluid-saturated materials rather than sulphide mineralization. Chargeability values in this profile range from approximately 134 msec to as low as 0.125 msec. This result demonstrates that not all conductive or fractured zones are mineralized, emphasizing the importance of integrating resistivity and chargeability data. Some fractures may be barren or filled with non-polarizable materials such as clay or groundwater.

Profile Six

Profile Six, located approximately 500 m from Profile Five and 200 m south of Profile Four, confirms the structural and mineralization trends observed in the area. A thick conductive zone ($<50 \Omega\text{m}$), extending beyond 70 m depth, exhibits correspondingly high chargeability values ($>400 \text{ msec}$) between depths of approximately 20 and 50 m. The lateral continuity of this anomaly between Profiles Four and Six suggests the presence of a persistent structural feature, likely a fracture corridor or shear zone, which acts as a conduit for hydrothermal fluid flow. The alignment of high chargeability zones across these profiles indicates a consistent mineralization trend, interpreted to be oriented approximately N-S to NW-SE. This reinforces the conclusion that mineralization within the Asu River Group is structurally controlled.

Conclusion

This study successfully applied integrated 2D Electrical Resistivity Tomography (ERT) and Induced Polarization (IP) to delineate subsurface characteristics and identify Pb-Zn mineralization targets in Ameka, within the Lower Benue Trough. The inversion results reveal that zones characterized by low resistivity ($10\text{-}50 \Omega\text{m}$) and high chargeability ($\geq 200 \text{ msec}$) are spatially associated with fractured and sheared intervals of the Asu River Group, indicating disseminated sulphide mineralization.

Four profiles (1, 3, 4, and 6) exhibit consistent signatures of mineralization at depths of approximately 17-50 m, whereas Profiles 2 and 5 show relatively high resistivity and low chargeability, suggesting compact, unfractured shale and absence of significant mineralization. The lateral continuity of conductive and highly chargeable zones particularly between Profiles 4 and 6 indicates a persistent structural corridor. Overall, the results demonstrate that mineralization in the study area is structurally controlled, occurring preferentially along fracture and shear zones that act as conduits for hydrothermal fluids. The integrated ERT-IP approach effectively reduces ambiguity inherent in single-parameter interpretation and provides a robust basis for target delineation in sedimentary-hosted Pb-Zn systems.

Recommendations

Targeted Drilling: Conduct confirmatory core drilling on Profiles 4 and 6 (high priority), followed by Profiles 1 and 3 (moderate priority), focusing on depths between 20-50 m where coincident low resistivity and high chargeability anomalies occur. **3D Geophysical Imaging:** Implement 3D ERT/IP surveys over the corridor defined by Profiles 4-6 to better resolve lateral continuity, geometry, and volume of the mineralized zones. **Geological and Geochemical Validation:** Integrate trenching, channel sampling, and assay analysis to validate geophysical anomalies and quantify ore grades (Pb, Zn, Ag).

Structural Mapping: Carry out detailed structural/lineament mapping to constrain fracture orientations (N-S to NW-SE)

controlling mineralization and to refine drill targeting. **Downhole Geophysics:** Where drilling is undertaken, apply downhole IP/resistivity logging to improve depth control and correlate surface anomalies with subsurface mineralization. **Environmental Baseline Studies:** Establish baseline hydrogeological and environmental assessments prior to large-scale exploration to support responsible resource development.

Author Contributions and Acknowledgement

This work was carried out in collaboration among all authors.

Luke Onyebuchi Nwakpa: Solely responsible for the conceptualization, study design, field data acquisition, data processing and inversion (ERT/IP), GIS integration, interpretation of results, and manuscript preparation.

Chikwendi N. Okereke: Provided academic supervision, guidance on methodology, and critical review of the manuscript.

F. B. Akiang: Co-supervision, technical guidance during data processing and interpretation, and review of the manuscript.

References

1. Hanor JS (2000) Barite–celestine geochemistry and environments of formation. *Reviews in Mineralogy and Geochemistry* 40: 193-275.
2. Nwajide CS (2013) *Geology of Nigeria's sedimentary basins*. CSS Press <https://virtuall.nln.gov.ng/resource/NLN-XAHR16DM8PVRJL6>.
3. Obaje NG (2009) *Geology and mineral resources of Nigeria*. Springer <https://link.springer.com/book/10.1007/978-3-540-92685-6>.
4. Nwachukwu SO (1972) The tectonic evolution of the southern portion of the Benue Trough, Nigeria. *Geological Magazine* 109: 411-419.
5. Reyment RA (1965) *Aspects of the geology of Nigeria*. University of Ibadan Press https://books.google.com.ng/books/about/Aspects_of_the_Geology_of_Nigeria.html?id=IbEJAQAIAAJ&hl=en.
6. Akande SO, Mücke A (1989) Mineralogy, texture, and paragenesis of the lead–zinc mineralization in the Lower Benue Trough, Nigeria. *Mineralium Deposita* 24: 156-162.
7. Telford WM, Geldart LP, Sheriff RE (1990) *Applied geophysics* (2nd ed.). Cambridge University Press <https://www.cambridge.org/gb/universitypress/subjects/earth-and-environmental-science/solid-earth-geophysics/applied-geophysics-2nd-edition>.
8. Dobrin MB, Savit CH (1988) *Introduction to geophysical prospecting* (4th ed.). McGraw-Hill <https://www.amazon.in/INTRODUCTION-GEOPHYSICAL-PROSPECTING-4ED-2017/dp/9339205227>.
9. Keller GV, Frischknecht FC (1966) *Electrical methods in geophysical prospecting*. Pergamon Press <https://catalogue.usask.ca/GEOL-482>.
10. Loke MH (2004) Tutorial: 2-D and 3-D electrical imaging surveys. Geotomo Software https://www.researchgate.net/publication/264739285_Tutorial_2-D_and_3-D_Electrical_Imaging_Surveys.